Assessment of the Clinical Relevance of *BRCA2* Missense Variants by Functional and Computational Approaches

Lucia Guidugli,[1,10] Hermela Shimelis,[1,10] David L. Masica,[2,10] Vernon S. Pankratz,[3] Gary B. Lipton,[4] Namit Singh,[5] Chunling Hu,[1] Alvaro N.A. Monteiro,[6] Noralane M. Lindor,[7] David E. Goldgar,[8] Rachel Karchin,[2,9] Edwin S. Iversen,[4] and Fergus J. Couch[1,*]

Many variants of uncertain significance (VUS) have been identified in *BRCA2* through clinical genetic testing. VUS pose a significant clinical challenge because the contribution of these variants to cancer risk has not been determined. We conducted a comprehensive assessment of VUS in the BRCA2 C-terminal DNA binding domain (DBD) by using a validated functional assay of BRCA2 homologous recombination (HR) DNA-repair activity and defined a classifier of variant pathogenicity. Among 139 variants evaluated, 54 had ≥99% probability of pathogenicity, and 73 had ≥95% probability of neutrality. Functional assay results were compared with predictions of variant pathogenicity from the Align-GVGD protein-sequence-based prediction algorithm, which has been used for variant classification. Relative to the HR assay, Align-GVGD significantly ($p < 0.05$) over-predicted pathogenic variants. We subsequently combined functional and Align-GVGD prediction results in a Bayesian hierarchical model (VarCall) to estimate the overall probability of pathogenicity for each VUS. In addition, to predict the effects of all other BRCA2 DBD variants and to prioritize variants for functional studies, we used the endoPhenotype-Optimized Sequence Ensemble (ePOSE) algorithm to train classifiers for BRCA2 variants by using data from the HR functional assay. Together, the results show that systematic functional assays in combination with *in silico* predictors of pathogenicity provide robust tools for clinical annotation of *BRCA2* VUS.

Introduction

Genetic testing of individuals with a family history of breast (MIM: 114480) and/or ovarian (MIM: 1677000) cancer has led to the identification of many unique *BRCA2* (MIM: 600185) variants of uncertain significance (VUS). The inability to assess the clinical relevance of VUS could deprive at-risk individuals of cancer-risk-management strategies—including enhanced cancer surveillance and screening and preventive prophylactic mastectomy and/or oophorectomy—available to carriers of known pathogenic *BRCA2* mutations. Similarly, VUS carriers diagnosed with metastatic breast or ovarian cancer might not benefit from therapy with platinum or PARP inhibitors targeting DNA-repair defects, as is currently recommended for individuals with *BRCA1* (MIM: 113705) or *BRCA2* pathogenic variants.[1–6]

The currently accepted method for classifying the clinical relevance of missense substitutions in *BRCA1* and *BRCA2* by the ENIGMA (Evidence-Based Network for the Interpretation of Germline Mutant Alleles) Consortium, which specializes in clinical classification of *BRCA1* and *BRCA2* variants—along with the NIH-supported ClinVar database of variants identified by genetic testing and the Global Alliance for Genomic Health (GA4GH) BRCA Exchange database of *BRCA1* and *BRCA2* variants, for which ENIGMA serves as an expert panel—is by a quantitative multifactorial probability-based model.[7–9] This model incorporates sequence alignment by the Align-GVGD sequence-based model for predicting the functional impact of missense variants, personal and family history of cancer, segregation of variants with cancer in families, co-occurrence of the variant with a known pathogenic mutation, population-based case-control analysis, and breast tumor pathological features.[8,10] The resulting posterior probabilities of pathogenicity are categorized into a five-tier clinical classification model similar to the American College of Medical Genetics and Genomics (ACMG) guidelines for disease-associated genes.

However, identification of germline *BRCA2* variants through clinical genetic testing and genome-wide tumor studies has far outpaced clinical annotation by the multifactorial model because of insufficient family-based genetic information for each VUS. Thus, there is a great need for scientifically rigorous alternative approaches for clinical annotation of *BRCA2* variants.[11,12] The ability to quantify the effects of specific genetic variants in a biological context makes model systems uniquely informative for studying genetic disease. To that end, the ACMG highlights *in vivo* and *in vitro* functional assays as being among

[1]Department of Laboratory Medicine and Pathology, Mayo Clinic, Rochester, MN 55905, USA; [2]Department of Biomedical Engineering and Institute for Computational Medicine, Johns Hopkins University, Baltimore, MD 21205, USA; [3]Division of Nephrology, University of New Mexico, Albuquerque, NM 87131, USA; [4]Department of Statistical Science, Duke University, Durham, NC 27708, USA; [5]Department of Structural Biology, University of California, San Diego, San Diego, CA 92093, USA; [6]Cancer Epidemiology Program, H. Lee Moffitt Cancer Center, Tampa, FL 33612, USA; [7]Department of Health Sciences Research, Mayo Clinic, Scottsdale, AZ 85259, USA; [8]Huntsman Cancer Institute and Department of Dermatology, University of Utah, Salt Lake City, UT 84132, USA; [9]Department of Oncology, Johns Hopkins University School of Medicine, Baltimore, MD 21218, USA
[10]These authors contributed equally to this work
*Correspondence: couch.fergus@mayo.edu
https://doi.org/10.1016/j.ajhg.2017.12.013.

the most robust for establishing the role of specific genetic variants in human health.[12] Thus, directly evaluating variants by using validated quantitative functional assays of BRCA2 activity could provide an alternative approach for VUS classification.

In this study, we performed a comprehensive functional analysis of variants encoding missense alterations in the BRCA2 DNA binding domain (DBD) (amino acids 2,460–3,170) by using a homology-directed DNA repair (HDR) assay.[13] We developed a statistical classifier yielding probabilities of pathogenicity for VUS on the basis of high sensitivity and specificity of the assay for established pathogenic missense mutations. We assessed the functional accuracy of the Align-GVGD *in silico* sequence-based prediction model by comparing it to the functional results and combined function-based and sequence-based probabilities of pathogenicity in VarCall, a computational tool that predicts the overall likelihood of pathogenicity for *BRCA2* VUS.[14] Finally, we used the endoPhenotype-Optimized Sequence Ensemble (ePOSE) algorithm[15] to train classifiers by using data from the HDR functional assays for the purpose of predicting the quantitative effect of any new variant in the BRCA2 DBD and to prioritize subsequent functional studies.[16,17]

Material and Methods

VUS Selection

A total of 139 *BRCA2*-encoded DBD missense variants (GenBank: NM_000059.3) identified in individuals receiving clinical genetic testing for *BRCA1* and *BRCA2* mutations were selected for this study in January 2013. Variants were identified through the ENIGMA, ClinVar, and BIC (Breast Cancer Information Core) databases and were selected to allow comparison of the HDR assay and Align-GVGD *in silico* prediction model categories. Between 10 and 13 VUS were randomly selected from each of five Align-GVGD C15–C55 categories,[9] 30 VUS were randomly selected from the C0 category (lowest probability of pathogenicity), and 51 VUS were randomly selected from the C65 category (highest probability of pathogenicity). The proportion of DBD missense variants accounted for by the selected variants in each Align-GVGD category in ClinVar (September 27, 2017) is shown in Table S1.

Align-GVGD Prediction

BRCA2 variants were assigned to Align-GVGD graded categories (C0–C65) and prior probabilities of pathogenicity ranging from 0.03 to 0.81 on the basis of an evolutionary protein sequence alignment ranging from *Homo sapiens* to *Strongylocentrotus purpuratus*.[9,18]

HDR Assay

Each variant was introduced into a 3X FLAG-tagged full-length *BRCA2* cDNA expression plasmid by site-directed mutagenesis. Variants were verified by Sanger sequencing. Co-transfection of *BRCA2* expression constructs and the iSce1 expression plasmid into DR-GFP *brca2*-deficient V-C8 cells was performed as described previously.[19–21] All variants were analyzed in duplicate in at least two independent clones. BRCA2 expression was verified by western blot, and transfection efficiency was measured by anti-FLAG immunofluorescence.[19–21] GFP-expressing cells were quantified by fluorescence-activated cell sorting (FACS). In GFP(+) cells, fold increases, which are equivalent to HDR-fold changes, were normalized and rescaled in relation to a 1:5 ratio derived from the p.Asp2723His pathogenic variant control and the neutral wild-type BRCA2 control.[21] All HDR assay results provided are based on the 1:5 scale.

HDR Statistical Classifier

At the time that these studies were completed, 12 variants in the DBD of BRCA2 had been categorized as class 1 known neutral variants (class 1 = neutral, posterior probability of pathogenicity ≤ 0.01), 21 variants had been classified as classes 1 and 2 combined (class 1/2) (class 2 = likely neutral, posterior probability = 0.01–0.049), and 13 variants had been categorized as class 4 and 5 (class 4/5) known pathogenic variants (class 4 = likely pathogenic, posterior probability = 0.95–0.99; class 5 = pathogenic, posterior probability ≥ 0.99) by a probability model that incorporates a family-based multifactorial likelihood model and prior probabilities of causality from the Align-GVGD sequence-based *in silico* prediction model (Table S1).[8,10] The sensitivity and specificity of the HDR assay were calculated on the basis of receiver operating characteristics (ROC) analysis[22] of the normalized HDR fold change for the class 4/5 and class 1 variants[21] (Supplemental Data). A statistical classifier based on a linear discriminant analysis (LDA) approach[23] was developed (Supplemental Data). A linear mixed model (LMM) was used for estimating the LDA model parameters. Posterior probabilities of pathogenicity for each VUS were derived via estimation of these means and variances of the distributions of the HDR results for the gold-standard class1 and class 4/5 variants[21] (Supplemental Material and Methods).

VarCall

VarCall is a Bayesian statistical model for VUS classification using functional assay data.[14] VarCall is structured as a two-component mixture model where one component describes the distribution of batch-adjusted log-ratio measurements from deleterious variants and the other describes the distribution of measurements from neutral (benign) variants. Each variant is accorded a prior probability of belonging to the "damaging" component, and Bayes' rule is used for estimating the posterior probability that the variant is from the sub-population of variants represented by that component. The 12 class 1 established neutral variants and 13 class 4/5 established pathogenic or likely pathogenic variants were accorded prior probabilities of being damaging of 0 and 1, respectively, and were used as a training set. The remaining VUS were accorded prior probabilities on the basis of the Align-GVGD algorithm.[9] A Markov chain Monte Carlo (MCMC) algorithm was used for inference. A sampler of 200,000 burn-in iterations followed by five million iterations was applied, and every 100th iteration was retained for inference. Marginal posterior means and standard deviations and intervals of the model parameters were calculated, and posterior probabilities of pathogenicity for each variant were formed.[24] A full description of the model and the MCMC analysis is provided in the Supplemental Data.

Classification Accuracy

The operating characteristics of the HDR and VarCall model predictions were estimated within a leave-one-out cross-validation framework. The models were re-estimated with each of the

training variants unlabeled (i.e., assumed to be a VUS) one at a time, and the posterior probability that each variant was pathogenic in the model was computed on the basis of a probability of pathogenicity ≥ 0.99 and a probability of neutrality ≤ 0.05. These predictions were compared with the known pathogenicity status of the variants, and the operating characteristics of the models were estimated (Supplemental Material and Methods).

Endophenotype-POSE

The Phenotype-Optimized Sequence Ensemble (POSE) algorithm is a bioinformatics method that builds classifiers specific to any trait and gene of interest.[15] The algorithm isolates subsets of sequences—from a pre-computed multiple-sequence alignment (MSA)—that optimize the classification of a training set of variants of known phenotypic impact. The utility of POSE has been extended to predict continuous-valued, quantitative traits (endophenotypes).[16,17] The endophenotype POSE (ePOSE) algorithm optimizes the sequence composition of an input MSA by iteratively maximizing the coefficient of determination (R^2 for regressing continuous-valued variables) between an internal score function and the variant-specific, continuous-valued endophenotypic measurements from a training set. The ePOSE score function considers conservation of amino acids and amino acid biophysical and biochemical properties and can optionally utilize 3D structural data. Scores from the ePOSE algorithm can take on any value from −3.0 to 3.0, where a score of zero is equivalent to the wild-type, scores from 0.0 to 3.0 indicate increasingly deleterious impact, and negative scores correspond to higher activity than the wild-type. In this study, we used the continuous-valued *BRCA2* HDR fold-change data in a leave-one-out cross-validation strategy to train an ePOSE classifier. We downloaded an initial MSA pool of 250 sequences from UniProt KB by submitting the sequence of human BRCA2 DBD. Predictions utilized a structural model of human BRCA2 DBD, which was previously built with MODELER 9.1.[25] The BRCA2 DBD missense variants that mapped onto the structure of the homology model were used for training and testing the ePOSE classifier in a leave-one-out cross-validation approach.

Results

Sensitivity and Specificity of the HDR Assay

HDR analysis of full-length BRCA2 proteins containing the 13 pathogenic and 12 non-pathogenic (neutral) standards was conducted in V-C8 cells (Table S1). Expression of full-length BRCA2 was verified by western blot (Figure S1). The mean normalized HDR results and standard errors (SEs) across all replicated experiments for each variant are presented on a 1–5 scale defined by the ratio of HDR fold change for the pathogenic p.Asp2723His variant and wild-type BRCA2. ROC curve analysis of the normalized mean HDR results for the established pathogenic and neutral variants identified HDR fold-change thresholds of <1.66 and <1.78, which correspond to 99% and 95% probabilities of pathogenicity, respectively, and HDR fold changes of >2.25 and >2.41 for 95% and 99% probabilities of neutrality, respectively (Table 1).

The sensitivity and specificity of the assay according to these standards were estimated at 100% (95% confidence interval [CI] = 75.3%–100% and 69.2%–100%, respectively). Extending to 21 class 1/2 and the 13 class 4/5 known standards also yielded sensitivity and specificity estimates of 100% (95% CI = 75.3%–100% and 82.4%–100%, respectively) (Table S1). Furthermore, based on family co-segregation data only, testing of 16 of these variants with ≥100:1 odds in favor of neutrality and nine variants with ≥20:1 odds in favor of pathogenicity gave similar sensitivity and specificity estimates of 100% (95% CI = 66.4%–100% and 76.8%–100%, respectively). Although other standards yielded smaller CIs, the class 1 and class 4/5 standards were selected as the most conservative gold standards for derivation of a statistical classifier and HDR-model-based probabilities of pathogenicity for all variants in the study (Table S2).[21]

An LDA statistical classifier based on the mean and variances of the distributions of the HDR results for the gold-standard (class 1 and class 4/5) variants was developed (Supplemental Material and Methods), and the probability of pathogenicity and neutrality for each VUS was estimated (Table 1; Table S2). A leave-one-out cross-validation analysis based on these variants yielded a sensitivity of 92.6% (95% CI = 78.7%–100%), a specificity of 92.6% (95% CI = 78.7%–100%), and classification rates for variants called neutral (≤5% probability of pathogenicity) of 96.2% (95% CI = 85.5%–100%) and for variants called deleterious (≥99% probability of pathogenicity) of 96.2% (95% CI = 85.5%–100%).

Functional Assessment of All VUS

Next, 105 additional VUS from the BRCA2 DBD were selected for HDR analysis. These were enriched with Align-GVGD categories C0 (prior probability of pathogenicity of 0.03) and C65 (prior probability of pathogenicity of 0.81) but also included variants from other Align-GVGD categories (C15–C55) (Table 1). To exclude the potential influence of these missense changes on mRNA splicing, we assessed all VUS with Human Splicing Finder 3.0 for effects on consensus splice sites, branch points, splice enhancer and silencer motifs, and the formation of *de novo* splice sites (Table S3). Variants p.Pro3039Leu and p.Arg2659Gly were predicted to disrupt consensus splice donor sites, p.Val2908Gly and p.Val2723Gly were predicted to create *de novo* donor splice sites, and p.Ser3123Gly was predicted to create a *de novo* splice acceptor site. Because these variants have little or only partial aberrant effects on splicing (Table S3),[26,27] they were included in the functional study.

A total of 41 VUS along with 13 known pathogenic variants substantially reduced the HDR activity of BRCA2, had ≥99% probability of pathogenicity, and were annotated as deleterious (Figure 1; Table 1). The positions of the variants with ≥99% probability of pathogenicity in the 3D structure of the BRCA2 DBD were evaluated. The majority were located at interfaces between the four globular clusters of this domain, although two were located in the BRCA2 tower structure (Figure S2). In contrast, 52 VUS and 21 known neutral variants had ≥95% probability of

Table 1. All BRCA2 Variants Evaluated

HGVS Amino Acid	HGVS cDNA	IARC Class	HDR Assay					Align-GVGD			VarCall		
			FC	SE	p(path)	p(neu)	Annotation	Class	Prior	95% CI	PrDel	logBF	Classification
p.Gly2748Asp	c.8243G>A	class 5	0.68	±0.07	1.000	2.96×10^{-12}	deleterious	C65	0.81	0.61–0.95	1.000	Inf	pathogenic
p.Leu2686Pro	c.8057T>C	–	0.72	±0.04	1.000	9.48×10^{-12}	deleterious	C45	0.66	0.34–0.93	0.994	4.407	pathogenic
p.Leu2653Pro	c.7958T>C	class 5	0.75	±0.08	1.000	3.39×10^{-11}	deleterious	C65	0.81	0.61–0.95	1.000	Inf	pathogenic
p.Arg3052Trp	c.9154C>T	class 5	0.86	±0.09	0.990	9.33×10^{-10}	deleterious	C65	0.81	0.61–0.95	1.000	Inf	pathogenic
p.Leu2721His	c.8162T>A	–	0.88	±0.10	1.000	1.70×10^{-9}	deleterious	C25	0.29	0.09–0.56	0.994	6.069	pathogenic
p.Arg2784Trp	c.8350C>T	class 3	0.91	±0.10	1.000	3.88×10^{-9}	deleterious	C65	0.81	0.61–0.95	1.000	4.730	pathogenic
p.Ala2603Pro	c.7807G>C	–	0.92	±0.6	1.000	4.78×10^{-9}	deleterious	C25	0.29	0.09–0.56	0.995	6.233	pathogenic
p.Asn3124Ile	c.9371A>T	class 4	0.92	±0.10	0.990	4.65×10^{-9}	deleterious	C65	0.81	0.61–0.95	1.000	Inf	pathogenic
p.Ser2670Leu	c.8009C>T	–	0.93	±0.07	1.000	6.19×10^{-9}	deleterious	C15	0.29	0.09–0.56	0.990	5.960	pathogenic
p.Leu2647Pro	c.7940T>C	class 4	0.93	±0.10	0.990	5.79×10^{-9}	deleterious	C65	0.81	0.61–0.95	1.000	Inf	pathogenic
p.Phe2562Leu	c.7684T>C	–	0.94	±0.05	1.000	8.20×10^{-9}	deleterious	C15	0.29	0.09–0.56	0.992	5.684	pathogenic
p.Gly3076Glu	c.9227G>A	–	0.95	±0.10	1.000	1.01×10^{-8}	deleterious	C65	0.81	0.61–0.95	0.998	4.966	pathogenic
p.Leu3125His	c.9374T>A	–	0.96	±0.07	1.000	1.36×10^{-8}	deleterious	C65	0.81	0.61–0.95	0.998	5.049	pathogenic
p.Lys2630Gln	c.7888A>C	–	0.98	±0.08	1.000	2.49×10^{-8}	deleterious	C45	0.66	0.61–0.95	0.972	2.868	pathogenic
p.Leu2510Pro	c.7529T>C	–	0.98	±0.11	1.000	2.61×10^{-8}	deleterious	C65	0.81	0.34–0.93	0.997	4.251	pathogenic
p.His2623Arg	c.7868A>G	–	1.00	±0.04	1.000	3.59×10^{-8}	deleterious	C25	0.29	0.09–0.56	0.995	6.172	pathogenic
p.Asp2723His	c.8167G>C	class 5	1.00	±0.01	0.990	3.81×10^{-8}	deleterious	C65	0.81	0.61–0.95	1.000	Inf	pathogenic
p.Ile2627Phe	c.7879A>T	class 5	1.01	±0.08	0.990	4.83×10^{-8}	deleterious	C15	0.29	0.09–0.56	1.000	Inf	pathogenic
p.Leu2688Pro	c.8063T>C	class 4	1.02	±0.08	0.990	5.81×10^{-8}	deleterious	C65	0.81	0.61–0.95	1.000	Inf	pathogenic
p.Gly3076Val	c.9227G>T	–	1.03	±0.11	1.000	8.07×10^{-8}	deleterious	C65	0.81	0.61–0.95	0.997	4.254	pathogenic
p.Gly3076Arg	c.9226G>C	–	1.03	±0.08	1.000	8.66×10^{-8}	deleterious	C65	0.81	0.61–0.95	0.999	5.090	pathogenic
p.Asp2723Val	c.8168A>T	–	1.04	±0.08	1.000	1.01×10^{-7}	deleterious	C65	0.81	0.61–0.95	0.997	4.363	pathogenic
p.Trp2788Arg	c.8362T>C	–	1.05	±0.08	1.000	1.37×10^{-7}	deleterious	C25	0.29	0.09–0.56	0.980	4.680	pathogenic
p.Trp2788Ser	c.8363G>C	–	1.06	±0.08	1.000	1.44×10^{-7}	deleterious	C35	0.66	0.61–0.95	0.990	3.970	pathogenic
p.Asp2723Ala	c.8168A>C	–	1.06	±0.11	1.000	1.49×10^{-7}	deleterious	C65	0.81	0.34–0.93	0.994	3.653	pathogenic
p.Phe2642Ser	c.7925T>C	–	1.07	±0.08	1.000	2.02×10^{-7}	deleterious	C45	0.66	0.61–0.95	0.993	4.351	pathogenic
p.Gly2609Val	c.7826G>T	–	1.07	±0.08	1.000	2.23×10^{-7}	deleterious	C65	0.81	0.34–0.93	0.997	4.430	pathogenic
p.Asp3095Glu	c.9285C>G	class 5	1.07	±0.12	0.990	1.89×10^{-7}	deleterious	C35	0.66	0.34–0.93	1.000	Inf	pathogenic

(*Continued on next page*)

Table 1. ***Continued***

HGVS Amino Acid	HGVS cDNA	IARC Class	HDR Assay					Align-GVGD			VarCall		
			FC	SE	p(path)	p(neu)	Annotation	Class	Prior	95% CI	PrDel	logBF	Classification
p.Thr2722Arg	c.8165C>G	class 5	1.08	±0.08	0.990	2.78×10^{-7}	deleterious	C65	0.81	0.61–0.95	1.000	Inf	pathogenic
p.Ser2691Phe	c.8072C>T	–	1.10	±0.06	1.000	4.08×10^{-7}	deleterious	C0	0.03	0.00–0.06	0.870	5.350	intermediate
p.Glu3002Lys	c.9004G>A	–	1.10	±0.08	1.000	4.35×10^{-7}	deleterious	C55	0.66	0.34–0.93	0.996	4.834	pathogenic
p.Asp2723Gly	c.8168A>G	class 5	1.11	±0.12	0.990	5.19×10^{-7}	deleterious	C65	0.81	0.61–0.95	1.000	Inf	pathogenic
p.Gly2596Glu	c.7787G>A	–	1.12	±0.09	1.000	5.77×10^{-7}	deleterious	C65	0.81	0.61–0.95	0.995	3.798	pathogenic
p.Gln2561Pro	c.7682A>C	–	1.13	±0.06	1.000	7.80×10^{-7}	deleterious	C15	0.29	0.09–0.56	0.986	5.166	pathogenic
p.Trp2626Cys	c.7878G>C	class 5	1.16	±0.13	0.990	1.56×10^{-6}	deleterious	C65	0.81	0.61–0.95	1.000	Inf	pathogenic
p.Gly2793Arg	c.8377G>A	–	1.18	±0.09	1.000	2.23×10^{-6}	deleterious	C65	0.81	0.61–0.95	0.998	4.833	pathogenic
p.Leu2792Pro	c.8375T>C	–	1.19	±0.09	1.000	3.03×10^{-6}	deleterious	C65	0.81	0.61–0.95	0.997	4.537	pathogenic
p.Gly2793Glu	c.8378G>A	–	1.19	±0.07	1.000	2.71×10^{-6}	deleterious	C65	0.81	0.61–0.95	0.998	4.913	pathogenic
p.Ala2786Pro	c.8356G>C	–	1.23	±0.09	1.000	5.96×10^{-6}	deleterious	C0	0.03	0.00–0.06	0.657	4.128	intermediate
p.Arg2784Gln	c.8351G>A	–	1.27	±0.14	1.000	1.46×10^{-5}	deleterious	C35	0.66	0.34–0.93	0.950	2.340	pathogenic
p.Gly2596Arg	c.7786G>C	–	1.28	±0.10	1.000	1.73×10^{-5}	deleterious	C65	0.81	0.61–0.95	0.988	2.953	pathogenic
p.Gly2585Arg	c.7753G>A	–	1.30	±0.10	1.000	2.47×10^{-5}	deleterious	C65	0.81	0.61–0.95	0.996	4.162	pathogenic
p.Gly3003Glu	c.9008G>A	–	1.33	±0.08	1.000	4.58×10^{-5}	deleterious	C65	0.81	0.61–0.95	0.987	2.896	pathogenic
p.Trp2725Leu	c.8174G>T	–	1.35	±0.10	1.000	6.72×10^{-5}	deleterious	C55	0.66	0.34–0.93	0.980	3.030	pathogenic
p.Gly2609Asp	c.7826G>A	class 4	1.35	±0.07	0.990	6.19×10^{-5}	deleterious	C65	0.81	0.61–0.95	1.000	Inf	pathogenic
p.Lys2498Glu	c.7492A>G	–	1.36	±0.10	1.000	7.99×10^{-5}	deleterious	C55	0.66	0.34–0.93	0.946	2.191	intermediate
p.Gln2655Arg	c.7964A>G	–	1.38	±0.09	1.000	1.13×10^{-4}	deleterious	C35	0.66	0.34–0.93	0.980	3.225	pathogenic
p.Tyr2726Cys	c.8177A>G	–	1.49	±0.16	0.999	7.87×10^{-4}	deleterious	C65	0.81	0.61–0.95	0.940	1.340	intermediate
p.Glu2847Lys	c.8539G>A	–	1.50	±0.12	0.999	9.24×10^{-4}	deleterious	C55	0.66	0.34–0.93	0.343	−1.314	intermediate
p.Gln2925Lys	c.8773C>A	–	1.51	±0.12	0.999	1.07×10^{-3}	deleterious	C45	0.66	0.34–0.93	0.683	0.104	intermediate
p.Asp3073Gly	c.9218A>G	–	1.52	±0.12	0.999	1.17×10^{-3}	deleterious	C65	0.81	0.61–0.95	0.980	2.425	pathogenic
p.Arg2659Gly	c.7975A>G	–	1.57	±0.12	0.997	2.57×10^{-3}	deleterious	C65	0.81	0.61–0.95	0.920	0.970	intermediate
p.Asp2611Gly	c.7832A>G	–	1.61	±0.12	0.995	0.005	deleterious	C65	0.81	0.61–0.95	0.879	0.531	intermediate
p.Tyr2660Asp	c.7978T>G	–	1.61	±0.12	0.995	0.005	deleterious	C65	0.81	0.61–0.95	0.910	0.810	intermediate
p.Leu2654Pro	c.7961T>C	–	1.66	±0.18	0.989	0.011	intermediate	C65	0.81	0.61–0.95	0.629	−0.922	intermediate
p.Leu2862Pro	c.8585T>C	–	1.67	±0.13	0.987	0.013	intermediate	C45	0.66	0.34–0.93	0.508	−0.630	intermediate

(*Continued on next page*)

Table 1. ***Continued***

HGVS Amino Acid	HGVS cDNA	IARC Class	HDR Assay					Align-GVGD			VarCall		
			FC	SE	p(path)	p(neu)	Annotation	Class	Prior	95% CI	PrDel	logBF	Classification
p.Arg2842Cys	c.8524C>T	–	1.68	±0.10	0.987	0.013	intermediate	C65	0.81	0.61–0.95	0.570	−1.180	intermediate
p.Glu3002Asp	c.9006A>T	–	1.75	±0.13	0.964	0.036	intermediate	C35	0.66	0.34–0.93	0.224	−1.906	intermediate
p.Ala2730Val	c.8189C>T	–	2.00	±0.10	0.480	0.520	intermediate	C0	0.03	0.00–0.06	0.027	−0.124	likely benign
p.Gly2812Glu	c.8435G>A	–	2.03	±0.11	0.390	0.610	intermediate	C65	0.81	0.61–0.95	0.139	−3.274	intermediate
p.Arg3007Gly	c.9019A>G	–	2.06	±0.13	0.320	0.680	intermediate	C45	0.66	0.34–0.93	0.100	−2.830	intermediate
p.Leu3011Pro	c.9032T>C	–	2.08	±0.13	0.270	0.740	intermediate	C25	0.29	0.09–0.56	0.058	−1.889	intermediate
p.Leu2972Trp	c.8915T>G	–	2.12	±0.10	0.190	0.810	intermediate	C15	0.29	0.09–0.56	0.088	−1.444	intermediate
p.Gly2837Glu	c.8510G>A	–	2.12	±0.13	0.180	0.820	intermediate	C65	0.81	0.61–0.95	0.091	−3.746	intermediate
p.Gln2925Arg	c.8774A>G	–	2.19	±0.14	0.091	0.90.9	intermediate	C35	0.66	0.34–0.93	0.096	−2.908	intermediate
p.Asp2606Gly	c.7817A>G	–	2.20	±0.17	0.082	0.918	intermediate	C65	0.81	0.61–0.95	0.151	−3.177	intermediate
p.Gly2584Asp	c.7751G>A	–	2.27	±0.17	0.038	0.962	likely neutral	C65	0.81	0.61–0.95	0.105	−3.597	intermediate
p.Tyr3092Ser	c.9275A>C	–	2.31	±0.10	0.025	0.975	likely neutral	C65	0.81	0.61–0.95	0.100	−3.690	intermediate
p.Tyr3035Ser	c.9104A>C	–	2.32	±0.10	0.025	0.975	likely neutral	C55	0.66	0.34–0.93	0.060	−3.430	intermediate
p.Arg2842His	c.8525G>A	class 1	2.36	±0.07	0.015	0.985	likely neutral	C25	0.29	0.09–0.56	0.000	−Inf	benign
p.Gln2925His	c.8775G>C	–	2.38	±0.18	0.012	0.988	likely neutral	C15	0.29	0.61–0.95	0.038	−2.335	likely benign
p.Thr3033Ile	c.9098C>T	–	2.38	±0.15	0.013	0.987	likely neutral	C65	0.81	0.09–0.56	0.070	−4.100	intermediate
p.Arg2488Ser	c.7464A>C	–	2.44	±0.19	7.11×10^{-3}	0.990	neutral	C35	0.66	0.34–0.93	0.021	−4.519	likely benign
p.Val2652Met	c.7954G>A	–	2.44	±0.11	6.76×10^{-3}	0.990	neutral	C15	0.29	0.09–0.56	0.040	−2.290	likely benign
p.Val2908Gly	c.8723T>G	class 2	2.44	±0.10	6.99×10^{-3}	0.990	neutral	C35	0.66	0.34–0.93	0.040	−3.980	likely benign
p.Pro2800Arg	c.8399C>G	–	2.46	±0.13	5.63×10^{-3}	0.990	neutral	C65	0.81	0.61–0.95	0.082	−3.861	intermediate
p.Arg2842Leu	c.8525G>T	–	2.47	±0.13	5.05×10^{-3}	0.990	neutral	C65	0.81	0.61–0.95	0.060	−4.250	intermediate
p.Leu2581Trp	c.7742T>G	–	2.53	±0.12	2.68×10^{-3}	0.990	neutral	C55	0.66	0.34–0.93	0.031	−4.091	likely benign
p.Gly2508Ser	c.7522G>A	–	2.56	±0.14	2.01×10^{-3}	0.990	neutral	C55	0.66	0.34–0.93	0.016	−4.774	likely benign
p.Pro2800Ser	c.8398C>T	–	2.64	±0.29	9.55×10^{-4}	0.990	neutral	C65	0.81	0.61–0.95	0.023	−5.203	likely benign
p.Ser2522Phe	c.7565C>T	–	2.73	±0.17	4.15×10^{-4}	1.000	neutral	C25	0.29	0.09–0.56	0.010	−4.040	likely benign
p.Arg2494Gln	c.7481G>A	–	2.89	±0.18	1.07×10^{-4}	1.000	neutral	C35	0.66	0.34–0.93	0.020	−4.820	likely benign
p.Arg2973Cys	c.8917C>T	class 1	2.90	±0.22	9.53×10^{-5}	0.990	neutral	C0	0.03	0.00–0.06	0.000	−Inf	benign
p.Arg2488Gly	c.7462A>G	–	2.92	±0.18	8.10×10^{-5}	1.000	neutral	C45	0.66	0.34–0.93	0.009	−5.420	benign

(*Continued on next page*)

Table 1. ***Continued***

HGVS Amino Acid	HGVS cDNA	IARC Class	HDR Assay					Align-GVGD			VarCall		
			FC	SE	p(path)	p(neu)	Annotation	Class	Prior	95% CI	PrDel	logBF	Classification
p.Val2969Met	c.8905G>A	class 1	3.01	±0.16	3.66×10^{-5}	0.990	neutral	C0	0.03	0.00–0.06	0.000	−Inf	benign
p.Ser2807Leu	c.8420C>T	–	3.04	±0.17	2.94×10^{-5}	1.000	neutral	C65	0.81	0.61–0.95	0.020	−5.360	likely benign
p.Leu2768His	c.8303T>A	–	3.40	±0.26	1.84×10^{-6}	1.000	neutral	C65	0.81	0.61–0.95	0.014	−5.698	likely benign
p.Ser3020Cys	c.9059C>G	–	3.48	±0.38	1.03×10^{-6}	1.000	neutral	C0	0.03	0.00–0.06	0.000	−6.220	benign
p.Asp2680Gly	c.8039A>G	–	3.53	±0.27	7.45×10^{-7}	1.000	neutral	C15	0.29	0.09–0.56	0.001	−6.115	benign
p.Val3081Ala	c.9242T>C	–	3.58	±0.22	5.26×10^{-7}	1.000	neutral	C25	0.29	0.09–0.56	0.000	−6.250	benign
p.Tyr3092Cys	c.9275A>G	class 2	3.62	±0.28	3.88×10^{-7}	1.000	neutral	C65	0.81	0.61–0.95	0.000	−6.750	benign
p.Arg2787Cys	c.8359C>T	–	3.63	±0.16	3.65×10^{-7}	1.000	neutral	C0	0.03	0.00–0.06	0.000	−6.500	benign
p.Ala2632Gly	c.7895C>G	–	3.68	±0.28	2.66×10^{-7}	1.000	neutral	C55	0.66	0.34–0.93	0.001	−7.275	benign
p.Ser3123Gly	c.9367A>G	–	3.72	±0.29	1.95×10^{-7}	1.000	neutral	C55	0.66	0.34–0.93	0.000	−7.060	benign
p.Ile2821Thr	c.8462T>C	–	3.76	±0.29	1.50×10^{-7}	1.000	neutral	C25	0.29	0.09–0.56	0.001	−6.374	benign
p.Leu2587Phe	c.7759C>T	–	3.77	±0.20	1.49×10^{-7}	1.000	neutral	C15	0.29	0.09–0.56	0.001	−6.197	benign
p.Phe2873Cys	c.8618T>G	–	3.79	±0.29	1.26×10^{-7}	1.000	neutral	C55	0.66	0.34–0.93	0.002	−6.709	benign
p.Leu2929Trp	c.8786T>G	–	3.85	±0.24	8.53×10^{-8}	1.000	neutral	C55	0.66	0.34–0.93	0.001	−7.815	benign
p.Ala2951Thr	c.8851G>A	class 1	3.87	±0.30	7.41×10^{-8}	0.990	neutral	C0	0.03	0.00–0.06	0.000	−Inf	benign
p.Gly2901Asp	c.8702G>A	–	3.89	±0.24	6.70×10^{-8}	1.000	neutral	C65	0.81	0.61–0.95	0.003	−7.402	benign
p.Glu3071Asp	c.9213G>T	–	3.95	±0.25	4.52×10^{-8}	1.000	neutral	C35	0.66	0.34–0.93	0.002	−7.135	benign
p.Ser2988Gly	c.8962A>G	–	3.97	±0.30	3.98×10^{-8}	1.000	neutral	C0	0.03	0.00–0.06	0.000	−6.570	benign
p.Arg2787His	c.8360G>A	class 2	3.97	±0.31	4.11×10^{-8}	1.000	neutral	C0	0.03	0.00–0.06	0.000	−7.420	benign
p.Pro2639Ala	c.7915C>G	–	3.98	±0.25	3.89×10^{-8}	1.000	neutral	C25	0.29	0.09–0.56	0.001	−6.077	benign
p.Lys2729Asn	c.8187G>T	class 1	3.99	±0.31	3.64×10^{-8}	0.990	neutral	C0	0.03	0.00–0.06	0.000	−Inf	benign
p.Ser2509Asn	c.7526G>A	–	4.05	±0.22	2.50×10^{-8}	1.000	neutral	C45	0.66	0.34–0.93	0.000	−7.620	benign
p.Ala2717Ser	c.8149G>T	class 1	4.08	±0.26	2.11×10^{-8}	0.990	neutral	C0	0.03	0.00–0.06	0.000	−Inf	benign
p.Leu2865Val	c.8593T>G	–	4.11	±0.45	1.68×10^{-8}	1.000	neutral	C25	0.29	0.09–0.56	0.001	−6.164	benign
p.Pro3039Leu	c.9116C>T	–	4.13	±0.32	1.48×10^{-8}	1.000	neutral	C0	0.03	0.09–0.56	0.000	−7.216	benign
p.Arg2991His	c.8972G>A	–	4.13	±0.20	1.51×10^{-8}	1.000	neutral	C25	0.29	0.00–0.06	0.000	−7.330	benign
p.Tyr3035Cys	c.9104A>G	–	4.16	±0.32	1.28×10^{-8}	1.000	neutral	C55	0.66	0.34–0.93	0.000	−8.230	benign
p.Pro3063Ser	c.9187C>T	class 2	4.21	±0.21	9.65×10^{-9}	1.000	neutral	C0	0.03	0.00–0.06	0.000	−7.571	benign

(*Continued on next page*)

Table 1. ***Continued***

HGVS Amino Acid	HGVS cDNA	IARC Class	HDR Assay					Align-GVGD			VarCall		
			FC	SE	p(path)	p(neu)	Annotation	Class	Prior	95% CI	PrDel	logBF	Classification
p.Pro2589His	c.7766C>A	class 2	4.25	±0.33	7.33×10^{-9}	1.000	neutral	C0	0.03	0.00–0.06	0.000	−6.851	benign
p.Ile2672Val	c.8014A>G	–	4.28	±0.08	6.02×10^{-9}	1.000	neutral	C15	0.29	0.09–0.56	0.000	−7.756	benign
p.Asp2679Gly	c.8036A>G	–	4.41	±0.28	3.08×10^{-9}	1.000	neutral	C65	0.81	0.61–0.95	0.002	−7.713	benign
p.Ala2466Val	c.7397C>T	class 1	4.46	±0.48	2.32×10^{-9}	0.990	neutral	C0	0.03	0.00–0.06	0.000	−Inf	benign
p.Asp3170Gly	c.9509A>G	class 1	4.50	±0.28	1.84×10^{-9}	0.990	neutral	C0	0.03	0.00–0.06	0.000	−Inf	benign
p.Arg2888Cys	c.8662C>T	class 1	4.52	±0.35	1.60×10^{-9}	0.990	neutral	C0	0.03	0.00–0.06	0.000	−Inf	benign
p.Lys2849Glu	c.8545A>G	–	4.56	±0.35	1.30×10^{-9}	1.000	neutral	C15	0.29	0.09–0.56	0.000	−7.463	benign
p.Asp2665Gly	c.7994A>G	class 2	4.56	±0.51	1.32×10^{-9}	1.000	neutral	C65	0.81	0.61–0.95	0.001	−8.096	benign
p.Glu2856Ala	c.8567A>C	class 1	4.57	±0.50	1.27×10^{-9}	0.990	neutral	C0	0.03	0.00–0.06	0.000	−Inf	benign
p.Glu2757Val	c.8270A>T	–	4.61	±0.35	9.79×10^{-10}	1.000	neutral	C35	0.66	0.34–0.93	0.000	−8.991	benign
p.Glu3152Lys	c.9454G>A	–	4.90	±0.38	2.24×10^{-10}	1.000	neutral	C0	0.03	0.00–0.06	0.000	−7.716	benign
p.Asp2913Glu	c.8739C>G	–	4.92	±0.38	2.02×10^{-10}	1.000	neutral	C35	0.66	0.34–0.93	0.000	−8.327	benign
p.Ser2782Asn	c.8345G>A	–	4.99	±0.38	1.38×10^{-10}	1.000	neutral	C45	0.66	0.34–0.93	0.000	−8.530	benign
p.Ala2851Val	c.8552C>T	–	5.03	±0.39	1.15×10^{-10}	1.000	neutral	C65	0.81	0.61–0.95	0.001	−8.513	benign
p.Arg2502Cys	c.7504C>T	–	5.04	±0.39	1.12×10^{-10}	1.000	neutral	C0	0.03	0.00–0.06	0.000	−7.890	benign
p.Gly2813Glu	c.8438G>A	–	5.09	±0.39	8.64×10^{-11}	1.000	neutral	C65	0.81	0.61–0.95	0.001	−8.553	benign
p.Arg2678Gly	c.8032A>G	–	5.12	±0.28	7.62×10^{-11}	1.000	neutral	C45	0.66	0.34–0.93	0.000	−9.010	benign
p.Val3079Ile	c.9235G>A	class 1	5.20	±0.41	5.02×10^{-11}	1.000	neutral	C0	0.03	0.00–0.06	0.000	−Inf	benign
p.Ser3058Gly	c.9172A>G	–	5.21	±0.40	4.89×10^{-11}	1.000	neutral	C0	0.03	0.00–0.06	0.000	−8.490	benign
p.Val2728Ile	c.8182G>A	–	5.29	±0.41	3.29×10^{-11}	1.000	neutral	C0	0.03	0.00–0.06	0.000	−7.950	benign
p.Asp2965His	c.8893G>C	class 2	5.33	±0.34	2.78×10^{-11}	1.000	neutral	C0	0.03	0.00–0.06	0.000	−8.404	benign
p.Lys2950Asn	c.8850G>T	class 2	5.41	±0.43	1.87×10^{-11}	1.000	neutral	C35	0.66	0.34–0.93	0.000	−8.814	benign
p.Glu2571Gly	c.7712A>G	–	5.50	±0.42	1.26×10^{-11}	1.000	neutral	C0	0.03	0.00–0.06	0.000	−8.204	benign
p.Tyr3098His	c.9292T>C	class 1	5.64	±0.15	6.90×10^{-12}	1.000	neutral	C0	0.03	0.00–0.06	0.000	−Inf	benign
p.Thr3013Ile	c.9038C>T	–	5.90	±0.45	2.23×10^{-12}	1.000	neutral	C0	0.03	0.00–0.06	0.000	−8.740	benign
p.Met2676Thr	c.8027T>C	class 2	5.90	±0.66	2.26×10^{-12}	1.000	neutral	C0	0.03	0.00–0.06	0.000	−8.294	benign
p.Ala3088Val	c.9263C>T	–	6.14	±0.47	8.44×10^{-13}	1.000	neutral	C0	0.03	0.00–0.06	0.000	−8.630	benign

GenBank: NM_000059.3. Abbreviations are as follows: FC, fold change in GFP(+) cells; SE, standard error; p(path), probability of pathogenicity; p(neu), probability of neutrality; prior, prior probability; PrDel, probability of deleteriousness; logBF, logBayes Factor; and –, data not available.

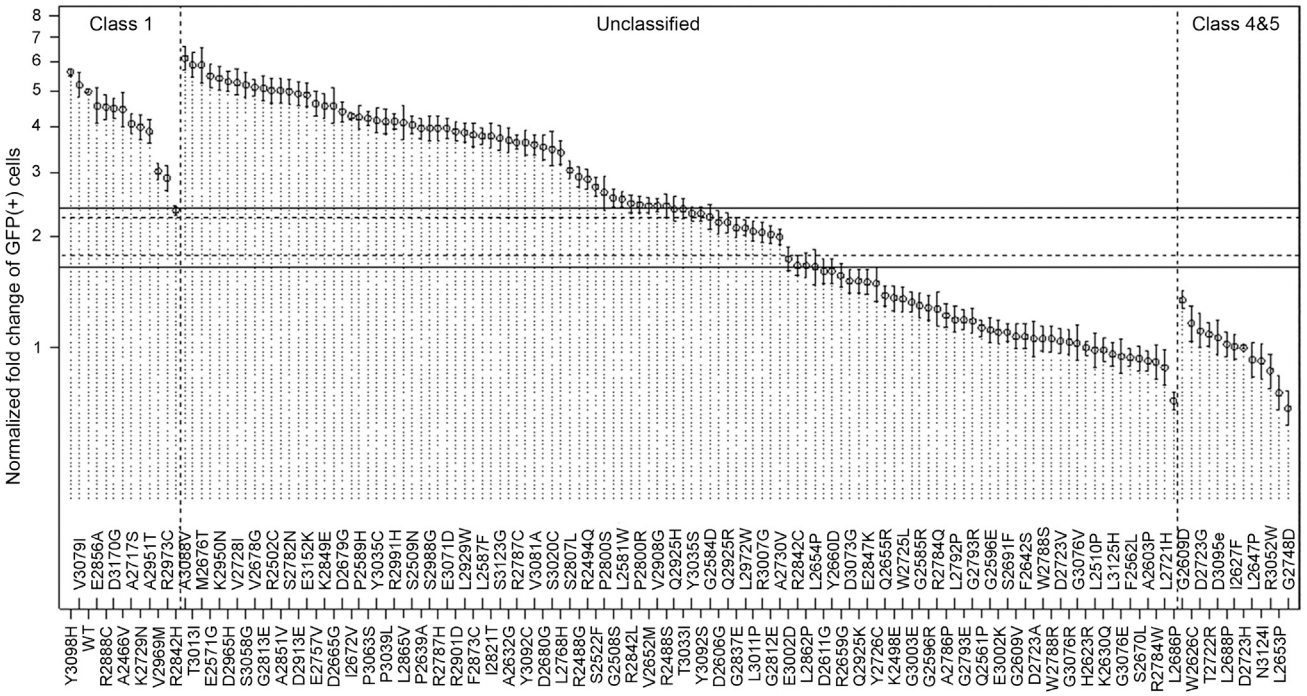

Figure 1. Influence of BRCA2-DBD Missense Variants on HDR Activity in Relation to Known Pathogenic and Neutral Variants Defined as Class 1, 4, or 5 in a Multifactorial Likelihood Model

The model-based HDR fold change with SE is displayed on a logarithmic scale for the class 1, unclassified, class 4, and class 5 variants. Solid lines represent 99% probability of pathogenicity and 99% probability of neutrality (fold increase in GFP(+) cells < 1.66 for deleterious variants and > 2.41 for neutral variants). Dotted lines represent 95% probability of pathogenicity and 95% probability of neutrality (fold increase in GFP(+) cells < 1.78 for deleterious variants and > 2.25 for neutral variants).

neutrality according to the HDR assay, and 47 VUS and 20 known neutrals had $\geq$99% probability of neutrality (Table 1). The variants with a probability of neutrality $\geq$ 99% were annotated as neutral, and the additional six variants with a probability of neutrality between 95% and 99% were annotated as likely neutral, consistent with the probability thresholds for neutral and likely neutral variants from the multifactorial likelihood classification model. Another 12 VUS had probabilities of pathogenicity ranging from 8.2% to 98.9% and were annotated as intermediate because the variants had intermediate or partial effects on BRCA2 function, and the correlation between intermediate activity and breast cancer risk is not defined (Table 1). The four VUS with probabilities of pathogenicity between 95% and 99% (p.Leu2654Pro, p.Leu2862Pro, p.Arg2842Cys, and p.Glu3002Asp) were included in this intermediate category because none of the known pathogenic standards displayed HDR activity below 99%. We observed little difference in VUS annotation when estimating 99% probability of pathogenicity and 95% probability of neutrality thresholds on the basis of the class 1/2 and class 4/5 dataset (Figure S3) and on family segregation data alone (Figure S4).

Correlation between Align-GVGD and HDR

Many sequence-based models for predicting whether missense mutations are deleterious or neutral have been developed. Among these, the Align-GVGD model has been used for estimating prior probabilities of pathogenicity for individual *BRCA1* and *BRCA2* missense substitutions on the basis of sequence conservation and physicochemical properties of the substitutions. Align-GVGD has been widely used for classifying *BRCA1* and *BRCA2* VUS in combination with a multifactorial likelihood model.[8] However, Align-GVGD prior probabilities for BRCA2 DBD missense variants are not always consistent with the classification by the multifactorial probability-based model (e.g., p.Ile2627Phe in C15: prior probability = 0.29, multifactorial posterior probability = 1.00, class 5) (Table S2). To further investigate the ability of Align-GVGD to predict the pathogenicity of BRCA2 VUS, we compared the annotation of DBD missense variants by the HDR functional assay with the Align-GVGD method (Tables 1 and 2; Table S4). Only a moderate correlation was observed (Spearman rank correlation = −0.495; 95% CI = −0.611 to −0.385). Examination of the distribution of p values for observed counts (HDR-classified variants) and predicted counts (Align-GVGD-classified variants) showed that the Align-GVGD categories associated with moderate (C35–C55) to high (C65) probability of pathogenicity were significantly different from the functional classification ($p = 0.0001$ and $p = 0.0009$, respectively) (Table 2; Figure 2; Table S4). Whereas Align-GVGD predicted that 66% of pooled C35–C55 VUS were deleterious, the HDR assay classified only 34% of VUS in this category as deleterious ($p = 0.0001$) (Table 2; Table S4). Similarly, 63% of C65

Table 2. Predicted Probability of Pathogenicity for BRCA2 Variants by Align-GVGD Category and HDR Assay

	Align-GVGD Categories (No. of Variants)			
	C0 (n = 30)	**C15–C25 (n = 23)**	**C35–C55 (n = 35)**	**C65 (n = 51)**
Classified by HDR				
Neutral	27	13	19	14
Intermediate	1	2	4	5
Deleterious	2	8	12	32
Proportion deleterious	0.07	0.35	0.34	0.63
95% CI	0.01–0.22	0.16–0.57	0.19–0.52	0.48–0.76
Predicted by Align-GVGD				
Prior Probability	0.03	0.29	0.66	0.81
Prior 95% CI	0.00–0.06	0.09–0.56	0.34–0.93	0.61–0.95
Predicted neutral	29.10	16.33	11.90	9.69
Predicted deleterious	0.90	6.67	23.10	41.31
p value	0.2391	0.54	0.0001[a]	0.0009[a]

[a]Align-GVGD prior probability differs significantly from the HDR classification.

were classified as deleterious by the HDR assay, whereas Align-GVGD predicted that 81% of C65 VUS were deleterious (p = 0.0009) (Table 2; Table S4). Align-GVGD categories with a lower probability of pathogenicity were more consistent with functional results, such that only p.Ala2786Pro, p.Ser2691Phe, p.Gln2561Pro, p.Ile2627Phe, p.Phe2562Leu, and p.Ser2670Leu from 41 Align-GVGD C0 and C15 variants were classified as deleterious by the HDR assay. Given the limited ability of Align-GVGD to accurately predict the pathogenicity of amino acid substitutions involving proline, the methods are highly correlated for variants with a low probability of pathogenicity. Overall, considering the high sensitivity and specificity of the HDR assay, these results suggest that the Align-GVGD model might over-predict the probability of pathogenicity for *BRCA2* VUS.

BRCA2 VarCall Prediction of Pathogenicity

Although the validated HDR functional assay can be useful for clinical VUS annotation, inclusion of other sources of evidence of pathogenicity or neutrality can provide greater confidence in the associated variant classification. Here, the VarCall two-component mixture model for VUS classification[14] was applied to 1,228 results from the BRCA2 HDR functional assay and to the probabilities of pathogenicity from the Align-GVGD sequence-based *in silico* prediction model that has been widely used for classifying *BRCA1* and *BRCA2* VUS (Supplemental Material and Methods).[8,9,21] The 12 known neutral variants and 13 known pathogenic variants were used as a training set. Under the VarCall model, each variant was accorded a prior probability of belonging to a "deleterious" component according to Align-GVGD,[9] and this was combined with a probability of pathogenicity derived from the HDR data under Bayes' rule for estimating the posterior probability that a variant was deleterious or neutral. Quantile-quantile plots of batch effects and standardized residuals from the VarCall model, averaged over the uncertainty in the posterior parameter, indicated that the model accurately describes residual variability (Figure S5). A leave-one-out cross-validation analysis of VarCall based on the 12 known neutral and 13 known pathogenic variants yielded a sensitivity of 92.6% (95% CI = 78.7%–100%), a specificity of 84.0% (95% CI = 64.6%–99.4%), and classification rates for variants called neutral (≤5% probability of pathogenicity) of 95.5% (95% CI = 82.9%–100%) and for variants called deleterious (≥95% probability of pathogenicity) of 96.2% (95% CI = 85.5%–100%) (Figure S5). Similar results were obtained with the class 1/2 and class 4/5 dataset (data not shown). Next, the performance of the VarCall model was assessed with seven additional non-conflicted pathogenic or likely variants and six non-conflicted benign or likely benign variants in ClinVar (Table S5). Importantly, these variants have not been classified by the ClinVar *BRCA1* and *BRCA2* expert panel with multifactorial models and were not used as initial standards in assessment of the HDR assay or Align-GVGD. Six of seven pathogenic or likely pathogenic variants had VarCall posterior probabilities of pathogenicity (pp) ≥ 0.95, whereas p.Tyr2660Asp had a pp = 0.91. In addition, all six benign or likely benign variants had VarCall a pp ≤ 0.05. Although the numbers are low, these findings suggest that VarCall correctly predicts variants as pathogenic and neutral.

When VarCall was applied to all 139 *BRCA2* variants, 45 were attributed a pp ≥ 0.95, including 36 with a pp ≥ 0.99 (Figure 3; Table 1). A further 68 had a pp ≤ 0.05, including 21 known neutral or likely neutral, whereas 26 variants had a pp = 0.05–0.95 (Figure 3; Table 1). All 45 variants with a VarCall pp ≥ 0.95 showed an HDR pp ≥ 0.99 (Table 1). In contrast, nine variants with an HDR

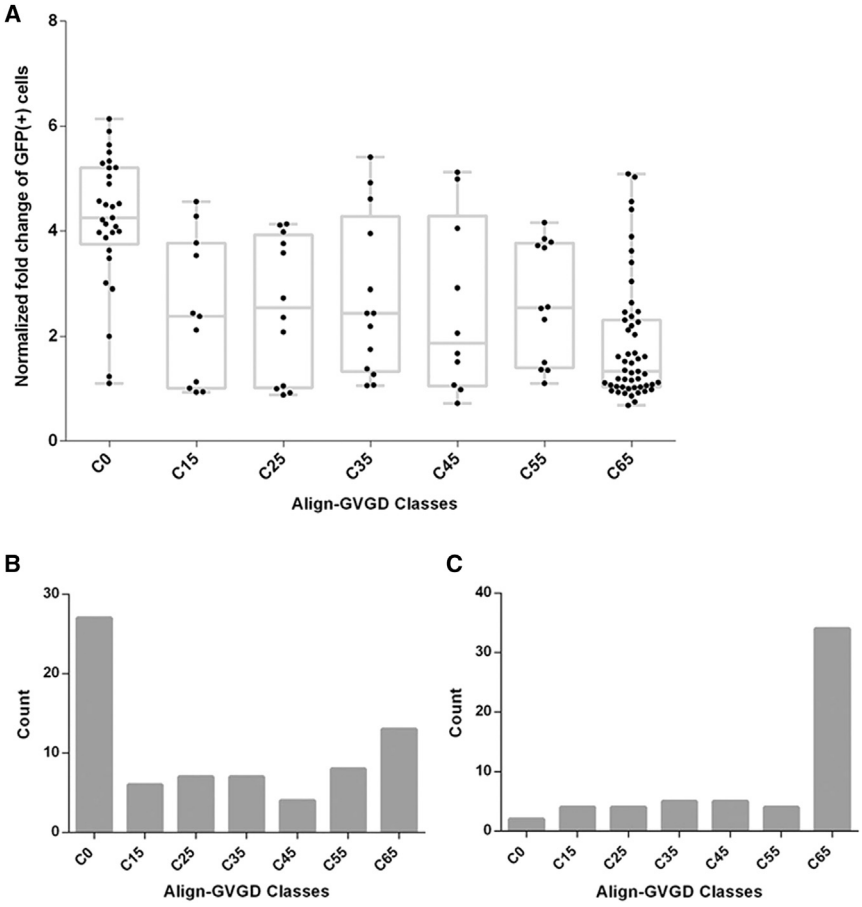

Figure 2. Comparison of HDR Activity and Align-GVGD Prediction for 139 BRCA2 Variants

(A) HDR normalized fold changes for 139 BRCA2-DBD missense changes are displayed for each of the seven Align-GVGD classification grades (C0–C65).

(B and C) 73 BRCA2-DBD missense changes with >95% probability in favor of neutrality (B) and 58 BRCA2-DBD missense changes with >95% probability in favor of pathogenicity (C) are displayed for each of the seven Align-GVGD classification grades (C0–C65).

pp ≥ 0.99 had a VarCall pp < 0.95 (Table 1) as a result of lower Align-GVGD prior probabilities (C0) or batch-to-batch variation in the HDR assay. Six of these had a VarCall pp ≥ 0.87, whereas p.Glu2847Lys, p.Gln2925Lys, and p.Ala2786Pro had a pp = 0.343–0.683. In addition, 67 of the 68 variants with a VarCall pp ≤ 0.05 also had an HDR pp ≤ 0.05. The p.Ala2730Val variant had a HDR pp = 0.48 but a VarCall pp = 0.027 because of a low Align-GVGD prior probability (C0) (Table 1). Conversely, 6 of 73 variants with an HDR pp ≤ 0.05 had a VarCall pp = 0.05–0.105 most likely because of high prior probabilities of pathogenicity (C55 = 0.66; C65 = 0.81).

To further evaluate the difference between the VarCall model and the HDR assay results, we directly combined the Align-GVGD prior probabilities of pathogenicity with the HDR-based probability of pathogenicity by using a Bayes model (Table S5), and we compared the composite HDR and Align-GVGD model with VarCall. The composite model showed high sensitivity and specificity similar to those of the HDR and VarCall models. All of the class 2 variants that were not used for developing any of these models showed a pp ≤ 0.05 for each of the three models (Table S5). In addition, three of the four variants with an HDR pp ≤ 0.05 but a VarCall pp > 0.05 had a composite pp > 0.05. Similarly, among the nine variants with an HDR pp ≥ 0.99 and a VarCall pp < 0.95, all had composite pp ≥ 0.99 (Table S5). The VarCall and composite models showed good correlation (r^2 = 0.85), and differences were mainly caused by variants with intermediate probabilities of pathogenicity.

On the basis of the results described above, variants with a VarCall pp ≥ 0.95 were conservatively classified as pathogenic, and VUS with a VarCall pp ≤ 0.05 were classified as benign or likely benign. Variants classified as pathogenic and variants classified as benign or likely benign with a VarCall pp ≥ 0.99 and pp ≤ 0.05, respectively, were consistent with classes 1, 2, and 5 from the International Agency for Research on Cancer (IARC) five-tier probability-based classification scheme for *BRCA2* VUS.[7] Variants with a VarCall pp = 0.05–0.95 were classified as intermediate rather than unclassified (IARC class 3) because the HDR assay indicated a partial reduction in BRCA2 DNA-repair activity. Overall, the VarCall model has excellent performance characteristics and is a viable option for combining functional results and Align-GVGD *in silico* prediction for reliable annotation of pathogenic *BRCA2* missense variants.

Correlation between ePOSE and HDR

Although the ACMG highlights *in vivo* and *in vitro* functional assays as important sources of data for establishing the role of specific genetic variants in human health, functional studies can be resource intensive. Thus, alternative methods for predicting the effects of variants on protein function are needed. The ePOSE algorithm was developed to train classifiers by using data from variant-specific functional assays (Figure S6). The classifiers can be used for predicting the quantitative effect of any new variant in the gene of interest and prioritizing subsequent functional studies.[16,17] Here, we used BRCA2 HDR fold-change results for 139 BRCA2 DBD variants in a leave-one-out cross-validation strategy to train ePOSE classifiers.

The HDR fold change and corresponding ePOSE score for each of the variants are shown in Table S6. The Pearson correlation between ePOSE scores and HDR fold changes

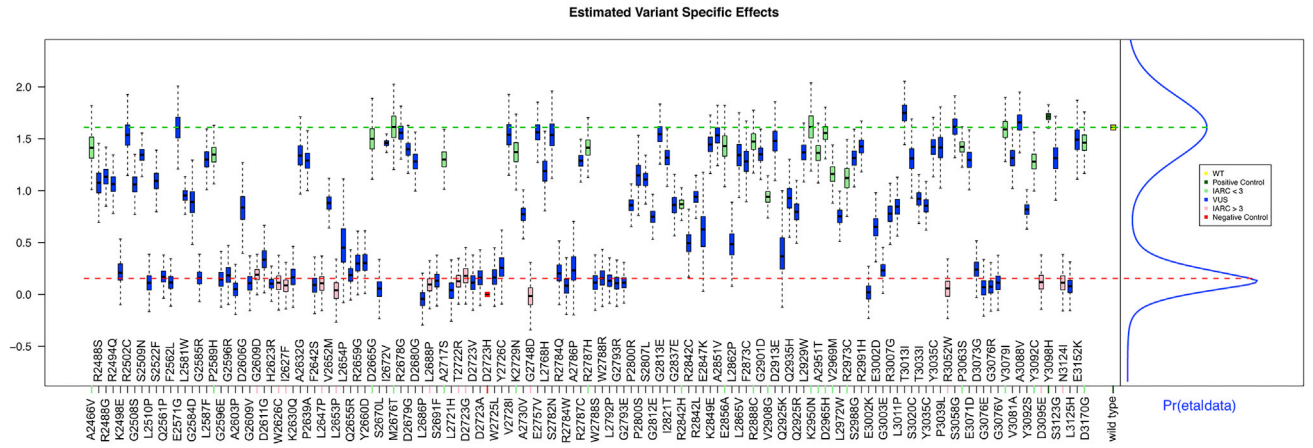

Figure 3. Plot of VarCall-Estimated Variant Effects Shows Individual Variants Plotted against HDR Activity
Variants are shown as the natural log of the normalized fold change in HDR activity. Error bars represent SE within individual measurements for each variant. The probability of pathogenicity (Pr(eta\data)) based on the lower pathogenic component and upper neutral component is plotted in the right-hand margin. The wild-type (WT), p.Tyr3098His positive controls, p.Asp2723His negative control, known pathogenic variants, known neutral variants, and VUS are color coded as indicated. Variants in green (IARC < 3) are classes 1 and 2. Variants shown in pink (IARC > 3) are classes 4 and 5.

was -0.68 (p value $= 7.4 \times 10^{-20}$), and the R^2 value was 0.46. Defining pathogenic and neutral variant classes with >95% probability of pathogenicity and ≥95% probability of neutrality (HDR fold-change cutoffs of 1.78 and 2.25, respectively) showed promising diagnostic performance of the ePOSE classifier. Specifically, the ePOSE classifier achieved a ROC area under the curve (AUC) of 0.87 and a sensitivity and specificity of 0.79 and 0.86, respectively (Table S7; Figure 4). Sensitivity and specificity were estimated for the ePOSE score that maximized balanced accuracy (arithmetic mean of sensitivity and specificity). The diagnostic performance of the ePOSE classifier improved for variants in the more extreme categories. For HDR fold-change cutoffs corresponding to >99% probability of pathogenicity and ≥99% probability of neutrality, the sensitivity and specificity for ePOSE were ≥0.80 (and the ROC AUC was 0.88), whereas categories based on an HDR fold change < 1.0 or > 5.0 yielded an ePOSE classifier ROC AUC of 0.97 and a sensitivity and specificity of 0.93.

Discussion

Accurate classification of the pathogenicity of variants is critical for the effective use of genetic testing results for clinical management. The many VUS identified in *BRCA2* by genetic testing cause significant clinical problems because of the lack of clarity regarding their contribution to breast, ovarian, and other cancers. Although multifactorial likelihood models of pathogenicity based on family and population-based approaches have been used for clinical annotation of VUS, especially by the ENIGMA *BRCA1* and *BRCA2* expert panel for ClinVar and the BRCA Exchange, the individual rarity of missense VUS prevents or delays classification of many additional VUS through these methods.[10,28] Thus, functional approaches that measure the impact of VUS on known biological processes and sequence-based predictive approaches represent alternative robust methods for clinical VUS annotation.

In this study, we evaluated the capability of a functional assay that measures the ability of VUS-containing BRCA2 proteins to repair a DNA double-strand break by homologous recombination to assess the pathogenicity of *BRCA2* VUS. The assay was applied to a total of 139 variants in the BRCA2 DBD. Using 34 known neutral and known pathogenic *BRCA2* variants, the HDR assay displayed 100% sensitivity and specificity, suggesting that the assay is a powerful method for clinical annotation of *BRCA2* VUS. Among the 105 VUS evaluated by the HDR assay, 41 showed ≥99% probability in favor of pathogenicity, and 52 had ≥95% probability in favor of neutrality. Given that only 13 *BRCA2* VUS are established as pathogenic by multifactorial models and are listed on the BRCA Exchange GA4GH BRCA Challenge website, and that only seven others are consistently identified as pathogenic on ClinVar, this represents a very substantial increase in the number of *BRCA2* VUS annotated as likely pathogenic. HDR thresholds for 99% probability of pathogenicity and 95% probability of neutrality (equating to 5% probability of pathogenicity) derived from these data could contribute to clinical annotation of any BRCA2 DBD VUS evaluated under the standardized conditions used for this assay.

VarCall was developed to incorporate two distinctly different methods for clinical annotation of *BRCA2* VUS in a complementary manner. The integration of two methods potentially accounts for any systematic inaccuracies in VUS annotation associated with either method. We applied the VarCall model to the 105 VUS along with the established pathogenic and neutral variants to estimate overall probabilities of pathogenicity. Using thresholds of

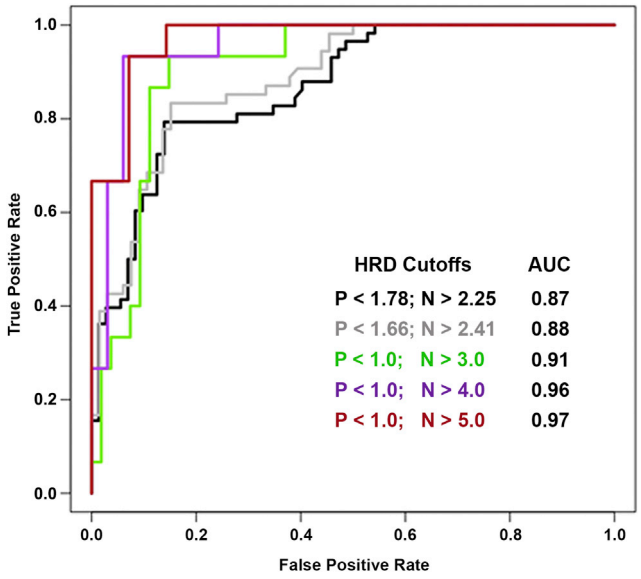

Figure 4. ROC Curves for the Continuous-Valued ePOSE Score and Variants Defined as Pathogenic or Neutral
For each of five variant groupings, *P* is the upper-bound HDR fold-change threshold for pathogenicity, and *N* is the lower-bound threshold for defining a variant as neutral. The color-coded inset shows the AUC at each of the five groupings.

95% and 5% probability of pathogenicity for pathogenic and benign variants, respectively, VarCall categorized 32 VUS as pathogenic and 47 as benign. Thus, the combination of the functional HDR assay and the Align-GVGD sequence-based method in the VarCall model provided classifications for 75% (79 of 105) of the VUS in this study. Because the VarCall model uses two forms of evidence for classification (function and *in silico* predictions) and provides more conservative evaluation of individual VUS than the HDR assay and *in silico* models alone, we propose that VarCall results are clinically relevant, and we classify variants evaluated by this model as pathogenic and benign (Table 1) in keeping with the terminology used by ENIGMA, ClinVar, and the BRCA Exchange. Overall, the HDR assay and the VarCall approach can dramatically reduce the number of non-informative results for VUS in the BRCA2 DBD. As more sources of data, such as the family-based and pathology-based information currently used in the ENIGMA multifactorial model, are integrated with functional data in VarCall and other complex models, it is expected that the number of VUS in *BRCA2* will be greatly reduced.

These studies also led to the identification of multiple VUS with intermediate functional effects. Specifically, 12 VUS that partially reconstituted BRCA2 HDR function had HDR-based probabilities of pathogenicity between 99% and 5%. However, when sequence-based prediction data were incorporated with functional data in the VarCall model, 26 VUS yielded probabilities of pathogenicity between the 5% and 95% VarCall thresholds. Further studies are needed to establish whether many of these variants represent hypomorphic variants with moderate effects on both cancer risk and function.[29–32] Interestingly, recent studies of p.Tyr3035Ser showed an association with moderate risks of breast cancer in a large case-control study (odds ratio = 2.4), which equates to an approximately 20% lifetime risk of breast cancer.[33] This variant had an HDR pp = 0.025 and a VarCall pp = 0.060, suggesting that any variant in the intermediate categories could be relevant to breast cancer risk, albeit at a lower penetrance than classical pathogenic protein-truncating mutations. Thus, additional efforts are needed to identify the activity and probability thresholds that reflect clinically relevant effects.

Many computational models such as SIFT and PolyPhen have been used for predicting whether missense variants are deleterious, neutral, or benign. Here, we used results from the HDR assay that exhibited 100% sensitivity and specificity for *BRCA2* pathogenic variants to assess the ability of the Align-GVGD computational model to predict deleterious variants in *BRCA2*. The substantial discrepancies observed between the HDR assay and Align-GVGD merit careful consideration because Align-GVGD has been used in combination with family-based data for clinical classification of *BRCA2* variants. Importantly, current classification models incorporating Align-GVGD require only limited data from family studies to classify an Align-GVGD C65 (prior probability = 0.81) VUS as a likely pathogenic variant (class 4, posterior probability > 0.95). Because the greatest discrepancy between the HDR assay and Align-GVGD was observed for Align-GVGD C45–C65 variants that were associated with prior probabilities of pathogenicity from 0.66 to 0.81, the suggestion is that the prior probabilities assigned to C45–C65 variants are too high. Recalibration of the prior probabilities for these categories of variants in BRCA2 should be considered. Perhaps Align-GVGD should contribute to the classification of VUS as pathogenic or likely pathogenic only when a substantial overall likelihood of pathogenicity is available from family, pathology, or other data sources or when it is combined with functional assay results, such as in VarCall. For this reason, we also validated the sensitivity and specificity of the HDR assay by using variants classified as pathogenic or neutral and family-based studies without Align-GVGD prior probabilities (Figure S4).

To further investigate clinical VUS annotation by using *in silico* sequence-based models, we trained classifiers for BRCA2 DBD variants in the ePOSE model by using the continuous quantitative measurements from the HDR assay. This approach offered an alternative sequence-based prediction approach to the binary measures of many algorithmic classifiers and the categorical approach of Align-GVGD. In a leave-one-out cross-validation strategy, continuous ePOSE scores were well correlated with the HDR fold-change values used for training, and comparing ePOSE scores with disease-relevant variant categories resulted in excellent diagnostic performance. However, because the observed performance resulted from training on data from a single study, expectations regarding classifier performance for new *BRCA2* variants should be tempered until further validation studies can be

completed. Perhaps the most immediate utility of the ePOSE classifier is for prioritizing additional *BRCA2* VUS for functional testing. Given the higher predictive value of the classifier at the lower and upper extremes of predicted HDR fold change, testing new variants in this category might be the most conservative test of the model, such that variants predicted to have an intermediate effect on HDR provide a greater challenge to model performance.

There are several possible limitations in the use of functional assays either alone or in combination with *in silico* prediction methods for clinical VUS annotation. Currently, the sensitivity and specificity of the HDR assay are based on relatively small numbers of established pathogenic missense variants. In addition, BRCA2 could have other functions, such as a role in protecting replication forks or regulating midbody structure in cytokinesis,[34,35] that influence cancer risks but are not effectively measured by the HDR assay. However, it should be noted that the HDR assay displays high sensitivity and specificity for known pathogenic variants and is strongly correlated with results for VUS that have been assessed by murine embryonic stem cell assays of cell survival and DNA-repair activity.[36–38] Ongoing studies have yet to determine whether the HDR assay, other functional studies, or VarCall can be applied to other regions of BRCA2. Importantly, the HDR assay and VarCall do not account for potential effects on stability or splicing, although splicing effects were considered in this study. Thus, fully calibrated splicing predictors will need to be incorporated into complex models for VUS annotation and classification in the future.

In summary, we have shown that the HDR functional assay is a robust tool for annotating *BRCA2* VUS within the DBD of BRCA2 and exceeds the sensitivity and specificity requirements of most clinical tests. The method is effective in combination with sequence-based predictors of pathogenicity in the VarCall model. This study supports the contention that functional studies in combination with sequence-based predictors can contribute to clinical classification of a large number of VUS in the absence of the family information currently used in multifactorial probability models of pathogenicity.

Supplemental Data

Supplemental Data include Supplemental Material and Methods, six figures, and seven tables and can be found with this article online at https://doi.org/10.1016/j.ajhg.2017.12.013.

Acknowledgments

This project was funded by a National Cancer Institute Specialized Program of Research Excellence (SPORE) in breast cancer at the Mayo Clinic (P50 CA116201), NIH grants CA116167 and CA192393, and the Breast Cancer Research Foundation.

Received: September 12, 2017
Accepted: December 18, 2017
Published: January 25, 2018

Web Resources

Align-GVGD, http://agvgd.hci.utah.edu/
BRCA Exchange, http://brcaexchange.org/
Breast Cancer Information Core, https://research.nhgri.nih.gov/bic/
ClinVar, https://www.ncbi.nlm.nih.gov/clinvar/
ENIGMA Consortium, https://enigmaconsortium.org/
GenBank, https://www.ncbi.nlm.nih.gov/genbank/
Human Splicing Finder 3.0, http://www.umd.be/HSF3/index.html
OMIM, http://www.omim.org

References

1. Evers, B., Drost, R., Schut, E., de Bruin, M., van der Burg, E., Derksen, P.W., Holstege, H., Liu, X., van Drunen, E., Beverloo, H.B., et al. (2008). Selective inhibition of BRCA2-deficient mammary tumor cell growth by AZD2281 and cisplatin. Clin. Cancer Res. *14*, 3916–3925.
2. Fong, P.C., Boss, D.S., Yap, T.A., Tutt, A., Wu, P., Mergui-Roelvink, M., Mortimer, P., Swaisland, H., Lau, A., O'Connor, M.J., et al. (2009). Inhibition of poly(ADP-ribose) polymerase in tumors from BRCA mutation carriers. N. Engl. J. Med. *361*, 123–134.
3. Audeh, M.W., Carmichael, J., Penson, R.T., Friedlander, M., Powell, B., Bell-McGuinn, K.M., Scott, C., Weitzel, J.N., Oaknin, A., Loman, N., et al. (2010). Oral poly(ADP-ribose) polymerase inhibitor olaparib in patients with BRCA1 or BRCA2 mutations and recurrent ovarian cancer: a proof-of-concept trial. Lancet *376*, 245–251.
4. Tutt, A., Robson, M., Garber, J.E., Domchek, S.M., Audeh, M.W., Weitzel, J.N., Friedlander, M., Arun, B., Loman, N., Schmutzler, R.K., et al. (2010). Oral poly(ADP-ribose) polymerase inhibitor olaparib in patients with BRCA1 or BRCA2 mutations and advanced breast cancer: a proof-of-concept trial. Lancet *376*, 235–244.
5. Gelmon, K.A., Tischkowitz, M., Mackay, H., Swenerton, K., Robidoux, A., Tonkin, K., Hirte, H., Huntsman, D., Clemons, M., Gilks, B., et al. (2011). Olaparib in patients with recurrent high-grade serous or poorly differentiated ovarian carcinoma or triple-negative breast cancer: a phase 2, multicentre, open-label, non-randomised study. Lancet Oncol. *12*, 852–861.
6. Sandhu, S.K., Schelman, W.R., Wilding, G., Moreno, V., Baird, R.D., Miranda, S., Hylands, L., Riisnaes, R., Forster, M., Omlin, A., et al. (2013). The poly(ADP-ribose) polymerase inhibitor niraparib (MK4827) in BRCA mutation carriers and patients with sporadic cancer: a phase 1 dose-escalation trial. Lancet Oncol. *14*, 882–892.
7. Plon, S.E., Eccles, D.M., Easton, D., Foulkes, W.D., Genuardi, M., Greenblatt, M.S., Hogervorst, F.B., Hoogerbrugge, N., Spurdle, A.B., Tavtigian, S.V.; and IARC Unclassified Genetic Variants Working Group (2008). Sequence variant classification and reporting: recommendations for improving the interpretation of cancer susceptibility genetic test results. Hum. Mutat. *29*, 1282–1291.
8. Lindor, N.M., Guidugli, L., Wang, X., Vallée, M.P., Monteiro, A.N., Tavtigian, S., Goldgar, D.E., and Couch, F.J. (2012). A review of a multifactorial probability-based model for classification of BRCA1 and BRCA2 variants of uncertain significance (VUS). Hum. Mutat. *33*, 8–21.
9. Tavtigian, S.V., Byrnes, G.B., Goldgar, D.E., and Thomas, A. (2008). Classification of rare missense substitutions, using

risk surfaces, with genetic- and molecular-epidemiology applications. Hum. Mutat. *29*, 1342–1354.

10. Goldgar, D.E., Easton, D.F., Deffenbaugh, A.M., Monteiro, A.N., Tavtigian, S.V., Couch, F.J.; and Breast Cancer Information Core (BIC) Steering Committee (2004). Integrated evaluation of DNA sequence variants of unknown clinical significance: application to BRCA1 and BRCA2. Am. J. Hum. Genet. *75*, 535–544.
11. MacArthur, D.G., Manolio, T.A., Dimmock, D.P., Rehm, H.L., Shendure, J., Abecasis, G.R., Adams, D.R., Altman, R.B., Antonarakis, S.E., Ashley, E.A., et al. (2014). Guidelines for investigating causality of sequence variants in human disease. Nature *508*, 469–476.
12. Richards, S., Aziz, N., Bale, S., Bick, D., Das, S., Gastier-Foster, J., Grody, W.W., Hegde, M., Lyon, E., Spector, E., et al.; ACMG Laboratory Quality Assurance Committee (2015). Standards and guidelines for the interpretation of sequence variants: a joint consensus recommendation of the American College of Medical Genetics and Genomics and the Association for Molecular Pathology. Genet. Med. *17*, 405–424.
13. Guidugli, L., Carreira, A., Caputo, S.M., Ehlen, A., Galli, A., Monteiro, A.N., Neuhausen, S.L., Hansen, T.V., Couch, F.J., Vreeswijk, M.P.; and ENIGMA consortium (2014). Functional assays for analysis of variants of uncertain significance in BRCA2. Hum. Mutat. *35*, 151–164.
14. Iversen, E.S., Jr., Couch, F.J., Goldgar, D.E., Tavtigian, S.V., and Monteiro, A.N. (2011). A computational method to classify variants of uncertain significance using functional assay data with application to BRCA1. Cancer Epidemiol. Biomarkers Prev. *20*, 1078–1088.
15. Masica, D.L., Sosnay, P.R., Cutting, G.R., and Karchin, R. (2012). Phenotype-optimized sequence ensembles substantially improve prediction of disease-causing mutation in cystic fibrosis. Hum. Mutat. *33*, 1267–1274.
16. Masica, D.L., Sosnay, P.R., Raraigh, K.S., Cutting, G.R., and Karchin, R. (2015). Missense variants in CFTR nucleotide-binding domains predict quantitative phenotypes associated with cystic fibrosis disease severity. Hum. Mol. Genet. *24*, 1908–1917.
17. Masica, D.L., and Karchin, R. (2016). Towards Increasing the Clinical Relevance of In Silico Methods to Predict Pathogenic Missense Variants. PLoS Comput. Biol. *12*, e1004725.
18. Tavtigian, S.V., Deffenbaugh, A.M., Yin, L., Judkins, T., Scholl, T., Samollow, P.B., de Silva, D., Zharkikh, A., and Thomas, A. (2006). Comprehensive statistical study of 452 BRCA1 missense substitutions with classification of eight recurrent substitutions as neutral. J. Med. Genet. *43*, 295–305.
19. Farrugia, D.J., Agarwal, M.K., Pankratz, V.S., Deffenbaugh, A.M., Pruss, D., Frye, C., Wadum, L., Johnson, K., Mentlick, J., Tavtigian, S.V., et al. (2008). Functional assays for classification of BRCA2 variants of uncertain significance. Cancer Res. *68*, 3523–3531.
20. Wu, K., Hinson, S.R., Ohashi, A., Farrugia, D., Wendt, P., Tavtigian, S.V., Deffenbaugh, A., Goldgar, D., and Couch, F.J. (2005). Functional evaluation and cancer risk assessment of BRCA2 unclassified variants. Cancer Res. *65*, 417–426.
21. Guidugli, L., Pankratz, V.S., Singh, N., Thompson, J., Erding, C.A., Engel, C., Schmutzler, R., Domchek, S., Nathanson, K., Radice, P., et al. (2013). A classification model for BRCA2 DNA binding domain missense variants based on homology-directed repair activity. Cancer Res. *73*, 265–275.
22. Fawcett, T. (2006). An introduction to ROC analysis. Pattern Recognit. Lett. *27*, 861–874.
23. McLachlan, G.J. (1992). Discriminant analysis and statistical pattern recognition (Wiley).
24. Gelfand, A., and Smith, A.F.M. (1990). Sampling-based approaches to calculating marginal densities. JASA *85*, 398–409.
25. Pieper, U., Webb, B.M., Dong, G.Q., Schneidman-Duhovny, D., Fan, H., Kim, S.J., Khuri, N., Spill, Y.G., Weinkam, P., Hammel, M., et al. (2014). ModBase, a database of annotated comparative protein structure models and associated resources. Nucleic Acids Res. *42*, D336–D346.
26. Walker, L.C., Whiley, P.J., Couch, F.J., Farrugia, D.J., Healey, S., Eccles, D.M., Lin, F., Butler, S.A., Goff, S.A., Thompson, B.A., et al.; kConFab Investigators (2010). Detection of splicing aberrations caused by BRCA1 and BRCA2 sequence variants encoding missense substitutions: implications for prediction of pathogenicity. Hum. Mutat. *31*, E1484–E1505.
27. Houdayer, C., Caux-Moncoutier, V., Krieger, S., Barrois, M., Bonnet, F., Bourdon, V., Bronner, M., Buisson, M., Coulet, F., Gaildrat, P., et al. (2012). Guidelines for splicing analysis in molecular diagnosis derived from a set of 327 combined in silico/in vitro studies on BRCA1 and BRCA2 variants. Hum. Mutat. *33*, 1228–1238.
28. Easton, D.F., Deffenbaugh, A.M., Pruss, D., Frye, C., Wenstrup, R.J., Allen-Brady, K., Tavtigian, S.V., Monteiro, A.N., Iversen, E.S., Couch, F.J., and Goldgar, D.E. (2007). A systematic genetic assessment of 1,433 sequence variants of unknown clinical significance in the BRCA1 and BRCA2 breast cancer-predisposition genes. Am. J. Hum. Genet. *81*, 873–883.
29. Monteiro, A.N., and Couch, F.J. (2006). Cancer risk assessment at the atomic level. Cancer Res. *66*, 1897–1899.
30. Lovelock, P.K., Spurdle, A.B., Mok, M.T., Farrugia, D.J., Lakhani, S.R., Healey, S., Arnold, S., Buchanan, D., Couch, F.J., Henderson, B.R., et al.; kConFab Investigators (2007). Identification of BRCA1 missense substitutions that confer partial functional activity: potential moderate risk variants? Breast Cancer Res. *9*, R82.
31. Spurdle, A.B., Healey, S., Devereau, A., Hogervorst, F.B., Monteiro, A.N., Nathanson, K.L., Radice, P., Stoppa-Lyonnet, D., Tavtigian, S., Wappenschmidt, B., et al.; ENIGMA (2012). ENIGMA–evidence-based network for the interpretation of germline mutant alleles: an international initiative to evaluate risk and clinical significance associated with sequence variation in BRCA1 and BRCA2 genes. Hum. Mutat. *33*, 2–7.
32. Spurdle, A.B., Whiley, P.J., Thompson, B., Feng, B., Healey, S., Brown, M.A., Pettigrew, C., Van Asperen, C.J., Ausems, M.G., Kattentidt-Mouravieva, A.A., et al.; kConFab; Dutch Belgium UV Consortium; German Consortium of Hereditary Breast and Ovarian Cancer; French COVAR group collaborators; and ENIGMA Consortium (2012). BRCA1 R1699Q variant displaying ambiguous functional abrogation confers intermediate breast and ovarian cancer risk. J. Med. Genet. *49*, 525–532.
33. Shimelis, H., Mesman, R.L.S., Von Nicolai, C., Ehlen, A., Guidugli, L., Martin, C., Calléja, F.M.G.R., Meeks, H., Hallberg, E., Hinton, J., et al.; for kConFab/AOCS Investigators; and for NBCS Collaborators (2017). BRCA2 Hypomorphic Missense Variants Confer Moderate Risks of Breast Cancer. Cancer Res. *77*, 2789–2799.
34. Schlacher, K., Christ, N., Siaud, N., Egashira, A., Wu, H., and Jasin, M. (2011). Double-strand break repair-independent

role for BRCA2 in blocking stalled replication fork degradation by MRE11. Cell *145*, 529–542.

35. Mondal, G., Rowley, M., Guidugli, L., Wu, J., Pankratz, V.S., and Couch, F.J. (2012). BRCA2 localization to the midbody by filamin A regulates cep55 signaling and completion of cytokinesis. Dev. Cell *23*, 137–152.
36. Kuznetsov, S.G., Liu, P., and Sharan, S.K. (2008). Mouse embryonic stem cell-based functional assay to evaluate mutations in BRCA2. Nat. Med. *14*, 875–881.
37. Kuznetsov, S.G., Chang, S., and Sharan, S.K. (2010). Functional analysis of human BRCA2 variants using a mouse embryonic stem cell-based assay. Methods Mol. Biol. *653*, 259–280.
38. Biswas, K., Das, R., Eggington, J.M., Qiao, H., North, S.L., Stauffer, S., Burkett, S.S., Martin, B.K., Southon, E., Sizemore, S.C., et al. (2012). Functional evaluation of BRCA2 variants mapping to the PALB2-binding and C-terminal DNA-binding domains using a mouse ES cell-based assay. Hum. Mol. Genet. *21*, 3993–4006.